Variable Refractive Index Polymer Thin Films Prepared by Plasma Copolymerization

H. Jiang,[†] K. O'Neill,[‡] J. T. Grant,[§] S. Tullis, K. Eyink, W. E. Johnson, P. Fleitz, and T. J. Bunning*

Air Force Research Laboratory, Materials and Manufacturing Directorate/MLP, Wright Patterson Air Force Base, Ohio 45433

Received November 26, 2003. Revised Manuscript Received January 26, 2004

We have developed plasma copolymerization techniques to fabricate photonic films with two (or more) monomers, whose composition can be controlled to manipulate the optical properties of the films. Spectroscopic ellipsometry confirmed that by changing monomer feed ratios (benzene and octafluorocyclobutane), films in the nanometer thickness range with refractive indices between those of the homopolymerized films could be fabricated. Spectroscopic analysis of the chemical structure of the copolymerized films using FTIR and XPS confirmed a nonlinear variation of chemical composition as a function of the monomer feed ratios. However, the refractive index of these films changes linearly with the film composition (characterized as the fluorine/carbon ratio). Facile control of optical thickness was demonstrated by fabricating multilayer antireflecting (AR) coatings on substrates of differing refractive indices. Very good agreement between the design and experimental spectra was obtained. This growth process creates a new way to prepare gradient-index (GRIN) films in the nanometer range, with a Δn greater than 0.3 and with well-controlled properties.

Introduction

Plasma-enhanced chemical vapor deposition (PECVD) is a unique technique to form nonconventional organic photonic films for a variety of electrical and optical applications.[1−9] Advantages of thin polymer films formed via the PECVD methodology include their dense and pinhole free internal morphology, hardness, optical transparency across the visible (400−700 nm) and NIR/SWIR (600 nm − 2 μm) regions, and environmental robustness. The deposition methodology can be applied to a variety of shapes and geometries including curved substrates, and it operates at low temperatures, is environment-friendly as no solvents are used, and can adopt a wide variety of organic monomers for deposition.

Recent work utilizing two monomers resulted in films with a large refractive index difference when individually plasma polymerized. By sequentially depositing each precursor to a $\lambda/4$ optical thickness, a multilayer stack exhibiting a reflection notch (stop band) at the design wavelength was formed.[10] Results from the experimental filter were in very good agreement (notch placement, width, and depth) with the designed filter.[10] However, simple alternating layer A−B−A−B filters suffer from many drawbacks including harmonics and side-lobes due to Fresnel reflections with the substrates. Both of these unnecessarily lower the overall transmission of any filter design. To overcome these limitations, both rugate and wavelet techniques to prepare complex, slowly varying (sinusoidal) refractive index modulations in films have been applied.[11−14] Advantages of these structures are increased transmission and better overall control of the optical notch depth and width.[15−17] To control optical thickness (the product of refractive index and physical thickness) of rugate and wavelet filters, the preparation of gradient index (GRIN) materials is the key. Furthermore, such optical devices are useful for many other applications and they are particularly

* To whom correspondence should be addressed. Phone: 937-255-3808, ext. 3167. Fax: 937-255-1128. E-mail: timothy.bunning@wpafb.af.mil.
[†] Anteon Corp., Dayton, OH 45431.
[‡] Now located at Pennsylvania State University, University Park, PA 16802.
[§] Research Institute, University of Dayton, Dayton, OH 45469.

(1) Hollahan, J. R.; Wydeven, T.; Johnson, C. C. *Appl. Opt.* **1974**, *13*, 1844.
(2) Reis, T. A.; Hiratsuka, H.; Bell, A. T.; Shen, M. In *Laser Induced Damage in Optical Materials*; NBS Special Publication 462; National Bureau of Standards, U.S. Government Printing Office: Washington, DC, 1976; p 230.
(3) Wydeven, T.; Kubacki, R. *Appl. Opt.* **1976**, *15*, 132.
(4) Chen, K. S.; Inagaki, N.; Katsuura, K. *J. Appl. Polym. Sci.* **1982**, *27*, 4655.
(5) Yasuda, H. *Plasma Polymerization*; Academic Press: Orlando, FL, 1985.
(6) d'Agostino, R., Ed. *Plasma Deposition, Treatment, and Etching of Polymers*; Academic Press: San Diego, CA, 1990.
(7) Klug, W.; Schneider, R.; Zöller, A. In *Optical Thin Films III: New Developments*; Seddon, R. I., Ed.; International Society for Optical Engineering (SPIE): San Diego, CA, 1990; Vol. SPIE 1323, p 88.
(8) Hrünwald, H.; Jung, M.; Kukla, R.; Adam, R.; Kunkel, S. *Surf. Coat. Technol.* **1997**, *93*, 99.
(9) Gong, X.; Dai, L.; Mau, A. W. H.; Griesser, H. J. *J. Polym. Sci., Part A: Polym. Chem.* **1998**, *36*, 633.
(10) Jiang, H.; Johnson, W. E.; Grant, J. T.; Eyink, K.; Johnson, E. M.; Tomilin, D. W.; Bunning, T. *Chem. Mater.* **2003**, *15*, 340.
(11) Delano, E. *J. Opt. Soc. Am.* **1967**, *57*, 1529−1533.
(12) Dobrowolski, J. A.; Lowe, D. *Appl. Opt.* **1978**, *17*, 3039.
(13) Southwell, W. H. *J. Opt. Sci. Am.* **1988**, *A5*, 1558.
(14) Fabricius, H. *Appl. Opt.* **1992**, *31*, 5191−5196. Fabricius, H. *Appl. Opt.* **1992**, *31*, 5216−5220.
(15) Johnson, W.; Southwell, W. H.; Hall, R. L. In *Optical Interference Coatings*; Optical Society of America: Tucson, AZ, 1995; Vol. 17, p 8.
(16) Baumeister, P. In *Optical Interference Coatings*; Optical Society of America: Tucson, AZ, 1995; Vol. 17, p 17.
(17) Hall, R. L. In *Optical Interference Coatings*; Optical Society of America: Tucson, AZ, 1995; Vol. 17, p 14.

10.1021/cm035226q CCC: $27.50
Published on Web 03/04/2004

important for polymeric nanophotonic devices with spatially varying optical thicknesses much less than the wavelength of light.[18−21] However, the use of these techniques for optical systems is currently restricted by fabrication limitations.[20,22,23] There are only a few flexible and environmentally friendly processes available that can fabricate large overall refractive index changes ($\Delta n > 0.1$) or control the profile shape. Particularly, realization of similar structures in polymeric-based films is difficult. Complex processing of polymer multilayers,[24] controlled photopolymerization,[25] and the use of block copolymers[26] coupled with anisotropic diffusion processes can potentially produce non A−B−A−B alternating structures; however, there is no simple control to tailor differences in either *n* or *d* layer to layer. Layer-by-layer deposition of alternating charged polyelectrolyte materials[27] may have the capability of controlling the optical thickness on the appropriate length scales but requires complex control equipment and wet chemistry techniques to fabricate photonic structures with many layers.

However, as described above, PECVD has the potential to be a simple and efficient method to fabricate structured polymer thin films with a priori control of the optical thickness variation. This paper documents the initial step to reach the goal of fabricating gradient photonic films with the PECVD copolymerization method. Namely, the growth of PECVD copolymerized films in the nano-thickness range with large (yet controllable) ranges of refractive indices ($\Delta n > 0.3$) was obtained by tuning the plasma copolymerization of two (or more) monomers with widely differing chemical structures. To demonstrate the versatility of this technique, optimized multilayer antireflection coatings have been deposited on a variety of substrates and the good match between experimental and design spectra indicates facile control of optical thickness.

Compared to plasma homopolymerization, plasma copolymerization is much more complicated because of interactions between the two (or more) monomers in all stages of the reaction process including initiation, growth, and deposition (film formation). In early work with benzene and octafluorocyclobutane (OFCB) monomers, regardless of the conditions and input OFCB feed rate employed, the plasma polymerized films contained no more than 3 atm % of fluorine as measured by XPS. In these cases, the feed positions of BOTH monomer gases were approximately 7 cm downstream from the plasma zone taking advantage of afterglow kinetics.[28,29] We speculate that in the afterglow reaction area, the lower dissociation energy barrier by opening the π bond of the C=C bond in benzene (about 2.74 eV), as compared to the C−F bond (5.35 eV) and C−C bond (3.61 eV), leads to a high reactivity of benzene molecules and preferentially facilitates the formation and interaction of aromatic excited species. On the basis of these considerations, two important changes were made in the work reported here. The first change was the relocation of the OFCB monomer inlet position relative to the plasma zone to facilitate OFCB monomer initiation. By introducing the OFCB monomer in the middle of the plasma zone, the formation of a large quantity of C_mF_n reactive species is guaranteed due to the much longer residence time in the plasma region. The second change was the replacement of the benzene mass flow controller with a manually adjusted high-accuracy metering valve in order to further decrease the benzene flow rate.

Experimental Section

The flowing afterglow reaction chamber system used for this study is similar to that described previously[10] except, as mentioned above, that the OFCB was introduced in the center of the plasma zone and the benzene flow rate was controlled with a manually adjusted, high-accuracy metering valve. Briefly, 50−200 standard cm^3/minute of 99.999% argon gas flowed into a 10-cm-diameter glass reactor at 0.5−2 Torr through a capacitively coupled, 13.56 MHz discharge. The argon was fed directly to the parallel plate electrodes supplying the primary discharge. Octafluorocyclobutane (OFCB, C_4F_8) was used as the low refractive index monomer, and was supplied by SynQuest Laboratories, Inc., as compressed gas, with a purity of 99%. OFCB (0.5−5 cm^3/min) was fed into the middle of the plasma zone between the two parallel-plate electrodes, controlled by a Sierra 902C flow controller. Vapor from HPLC grade (99.9% purity) benzene supplied by Aldrich Co. was used as the high-refractive index monomer. The vapor was introduced into the chamber 7 cm downstream from the plasma zone, and the benzene reservoir was maintained at 19.0 ± 0.1 °C by a water-bath thermostat. The flow rate of benzene vapor was controlled between 0.001 and 0.5 CC/min by a manually adjusted high-accuracy metering valve. When the benzene vapor flow rate was over 1 CC/min, a Sierra 902C flow controller replaced the metering valve. Both monomers were used as received without any further purification. The resultant plasma homopolymerized (PP-)benzene films had refractive indices ranging from 1.62 to 1.68, while the PP-−OFCB films had refractive indices ranging from 1.35 to 1.39 over the 700−400 nm spectral region.

Plasma polymerized films were deposited directly on potassium bromide (KBr) disks in the reaction chamber for subsequent Fourier transform infrared (FTIR) analysis, which was performed on a Perkin-Elmer Spectrum 2000 FTIR spectrometer in the transmission mode. A range of 400 to 4000 cm^{-1} was scanned 128 times in 1 cm^{-1} increments and averaged.

XPS analysis was carried out in a Surface Science Instruments M-Probe using monochromatic Al Kα X-rays. The surface composition was measured from survey scans taken with an analyzer pass energy of 150 eV and with a binding energy range of 0 to 1000 eV. The fluorine and carbon concentrations were measured from the F 1s and C 1s peak areas, and then corrected for ionization cross-sections and analyzer transmission using ESCAVB software from Service Physics . Measurements were also taken of the C 1s line-shape at a pass energy of 100 eV (higher energy resolution) to

(18) Yamazaki, H.; Asano, Y. *J. Appl. Phys.* **1982**, *21*, L673.
(19) Osada, Y. *Membrane (Japanese)* **1985**, *10*, 215.
(20) Gomez-Reino, C.; Perez, M. V.; Bao, C. *Gradient-Index Optics, Fundamentals and Applications*; Springer: Berlin, Germany, 2002.
(21) Lekishvili, N.; Nadareishvili, L.; Zaikov, G.; Khananashvili, L. *Polymers and Polymeric Materials for Fiber and Gradient Optics*; VSP: Utrecht, 2002.
(22) Houde-Walter, S. In *Gradient-Index Optics and Miniature Optics*; SPIE 935; The International Society for Optical Engineering: Bellingham, WA, 1988; Vol. 935, p 2.
(23) Samuels, J. E.; Moore, D. T. *Appl. Opt.* **1990**, *29*, 4042.
(24) Weber, M. F.; Stover, C. A.; Gilbert, L. R.; Nevitt, T. J.; Ouderkirk, A. J. *Science* **2000**, *287*, 2451.
(25) Weber, A. M.; Smothers, W. K.; Trout, T. J.; Michkish, D. J. In *Practical Holography IV*; SPIE 1212; The International Society for Optical Engineering: Bellingham, WA, 1990; Vol. 1212, p 30.
(26) Edrington, A. C.; Urbas, A. M.; Derege, P.; Chen, C. X.; Swager, T. M.; Hadjichristidis, N.; Xenidou, M.; Fetters, L. J.; Joannopoulos, J. D.; Fink, Y.; Thomas, E. L. *Adv. Mater.* **2001**, *13*, 421.
(27) Hiller, J.; Mendelson, J. D.; Rubner, M. F. *Nat. Mater.* **2002**, *1*, 59.
(28) Haaland, P. D.; Targove, J. *Appl. Phys. Lett.* **1992**, *61*, 34.
(29) Haaland, P. D.; Ibrani, S.; Jiang, H. *Appl. Phys. Lett.* **1994**, *64*, 1629.

Table 1. Monomer Feed Rates, Feed Ratios, Fluorine/Carbon Ratios, and Deposition Rates of PECVD Copolymer Films

sample	OFCB feed rate F (CC/min)	benzene feed rate C (CC/min)	monomer feed ratio $B/(B+F)$	fluorine/carbon atomic ratio (F/C) in the film[a]	film deposition rate (nm/min)
PP-benzene	0	0.18	1.00	0	8.7
Copolymer film BF9	0.5	0.18	0.150	0.23	34.0
Copolymer film BF8	2.5	0.18	0.0672	0.46	41.7
Copolymer film BF7	3	0.18	0.0566	0.47	36.8
Copolymer film BF6	3	0.079	0.0257	0.60	34.8
Copolymer film BF5	3	0.040	0.0132	0.62	29.7
Copolymer film BF4	3	0.013	0.0043	0.81	21.2
Copolymer film BF3	3	0.012	0.0040	0.96	17.0
Copolymer film BF2	3	0.010	0.0033	1.25	11.0
Copolymer film BF1	3	0.004	0.0013	1.36	8.7
PP-OFCB	3	0	0	1.62	3.3

[a] Determined by XPS.

distinguish the different carbon chemistries in the films. The curve-fitting procedures will be discussed elsewhere.

The refractive index, absorption coefficient, and film thickness were determined by ellipsometry using a Woollam variable angle spectroscopic ellipsometer system including a VB-200 ellipsometer control module and a CVI Instruments DigiKröm 242 monochromator with 100 W mercury/75 W xenon light sources. All data analysis was performed using Windows version 3.352 WVASE32 software. The Urbach−Sellmeier model (eq 1) for the polymer film over a Si substrate was used to determine the refractive index, the absorption coefficient, and the film thickness.

$$n = \sqrt{A + \frac{B\lambda^2}{(\lambda^2 - C^2)} + \frac{D\lambda^2}{(\lambda^2 - E^2)}}$$

$$k = F\lambda e^{-G[1/H - 1/\lambda]} \qquad (1)$$

In these equations, n is the refractive index, k is the extinction coefficient, λ is the wavelength, and $A-H$ are constants. Profilometry was used to measure film thickness for comparison to the corresponding ellipsometry data. Results were consistent to within 5%. In this paper, the refractive index at 632.8 nm was used for comparison.

To test this approach for fabricating gradient photonic films, AR coatings were grown using multiple-layer PECVD copolymer films to simulate the gradient coatings. The design strategy was to change the coating from that of the refractive index of the substrate to the lowest refractive index possible using the plasma copolymerized films. The refractive index function for the coating could be linear, sinusoidal, cubic, or quintic,[30] and a quintic-type function was used here, but was approximated with steps in the refractive index. Any conventional thin film coating software package can be applied to calculate the spectral performance for these coatings. For this effort, the optical performance of the theoretical designs was performed using Tony Noe's TFCalc software package (Software Spectra, Inc.).

The transmittance spectra of all films deposited on BK-7 and F2 glasses and quartz substrates were measured with a Cary 500 Scan UV−Vis−NIR spectrophotometer (Varian) in the wavelength range of 400−700 nm.

Results and Discussion

Nine different copolymerized films, each formed using different feed compositions, in addition to the homopolymerized films were examined in the new reaction design and details are listed in Table 1. The deposition rate of the plasma copolymer films increased with benzene share, but was also affected by the total amount of monomers fed. The individual OFCB and benzene feed rates, designated as F and B respectively, are given in Table 1. The monomer feed ratio used in this paper is defined as that of benzene to the total, i.e., $B/(B + F)$, and is also listed in the table. The chemical variation of the nine copolymerized films was examined with FTIR and XPS. Encouragingly, the feed ratio exerts a significant influence on the chemical structure as shown in Figures 1−3.

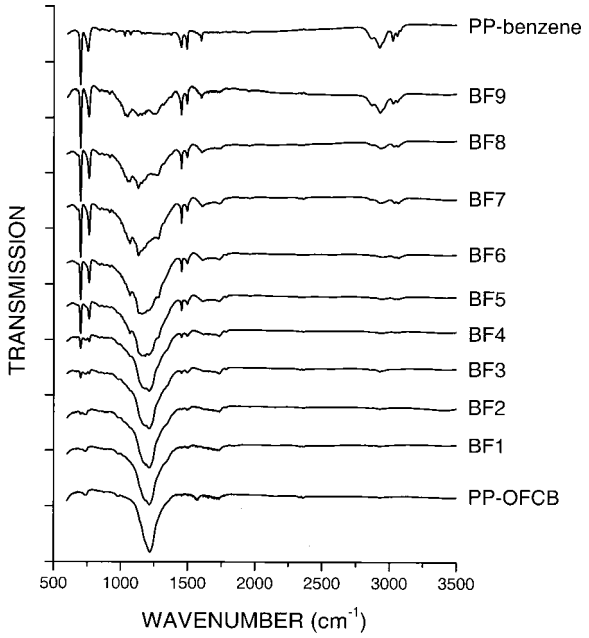

Figure 1. FTIR spectra of homopolymerized benzene (top) and OFCB (bottom) films. Spectra from bottom to top are from films formed using an increasing $B/(B + F)$ feed ratio. The spectra are normalized and offset for clarity.

The changes in chemical composition of the plasma copolymer films with the feed ratio are substantiated by their FTIR spectra, as shown in Figure 1. The bottom curve is the FTIR spectrum of the OFCB homopolymer film and the top one is that of the benzene homopolymer film. Between these two are the FTIR spectra of the plasma copolymer films, with a progressive increase in the feed volume ratio, reading from bottom to top. In the FTIR spectrum of the OFCB homopolymer film, a comparatively broad band in the range of about 980 to 1450 cm^{-1} is due to a convolution of C_mF_n and $(C_mF_n)_x$ vibration modes. The lack of any distinction between the individual fluorine species' vibration modes suggests that this film has a highly amorphous and disordered structure.[10,31] In the FTIR spectrum of the benzene homopolymer film (top curve), the peaks in the 3000−

(30) Southwell, W. H. U.S. Patent 4,583,822, 1986.

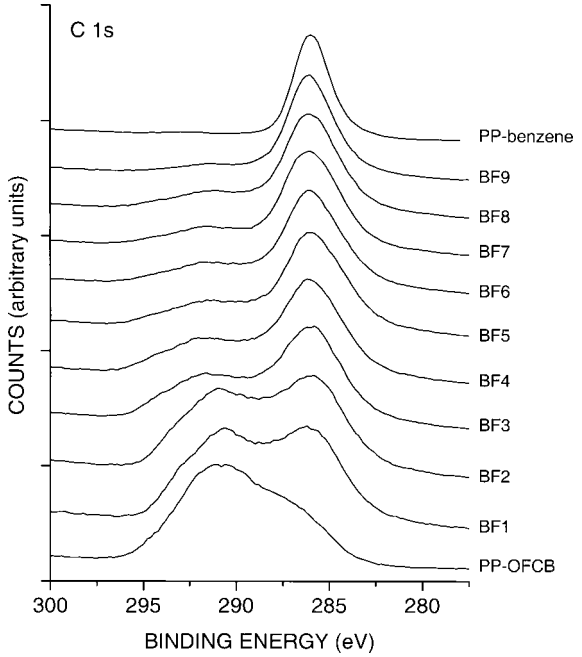

Figure 2. C 1s XPS spectra of homopolymerized benzene (top) and OFCB (bottom) films. Spectra from bottom to top are from films formed using an increasing $B/(B + F)$ feed ratio. The spectra are normalized and offset for clarity.

3100 cm^{-1} region such as 3057, 3081, and 3096 cm^{-1}, correspond to aromatic C−H stretching.[32−34] Further evidence of benzene ring retention can be seen by the out-of-plane aromatic C−H deformation (γ) at 754 cm^{-1} and aromatic ring (C═C) rocking motion (δ) at 699 cm^{-1}.[32−34] The peaks at 1494 and 1599 cm^{-1}, corresponding to C═C ring stretching in $-C_6H_5$, indicate C═C conjugated and nonconjugated stretchings caused by substitutions on the phenyl rings or ring opening upon plasma polymerization.[32,33,35] In addition, there are aliphatic C−H stretching modes at 2800−3000 cm^{-1}, such as 2867 cm^{-1} due to methyl groups and 2925 cm^{-1} due to methylene groups. Also, the band at 1452 cm^{-1} denotes the C−H bending in CH_2 and CH_3. These results suggest that part of the benzene ring is broken during the plasma reaction to form various aliphatic moieties.

XPS measurements further confirm the variations in the chemical structure as indicated by fluorine/carbon (F/C) atomic ratios listed in Table 1. As the feed ratio increases, the total fluorine amount determined by XPS in the resultant plasma copolymer films continually decreases (F/C ratio decreases). Note that the F/C ratio of the OFCB monomer is 2, but all the PECVD polymer films have lower F/C ratios, indicating significant defluorination during the growth. Figure 2 shows the change of the XPS C 1s spectra of the resultant plasma homo/copolymer films with feed ratio. At the bottom is the spectrum of an OFCB homopolymerized film, followed by the spectra of the plasma copolymer films with increasing B/F feeding ratio from bottom to top. The top spectrum is from the benzene homopolymerized film. This plot discloses that the plasma reactions induced the formation of various fluorine species, such as C_mF_n and $(C_mF_n)_x$, including CF, CF_2, and CF_3, and these species experienced obvious changes during the plasma homo/copolymerization. It also gives an intuitive image of the growth and the change of many other carbon components, including C−C, C═C, and $CH_{i(i=1-3)}$, as indicated in the IR spectra. As seen in the spectra, from bottom to top, with increasing $B/(B + F)$ feed ratio during the plasma copolymerization, the amount of C_mF_n species in the resultant films gradually decrease, while the other carbon components increase.

The XPS and IR measurements draw a clear picture of the variations of the composition and structure of the plasma homo/copolymer films of OFCB and benzene. First, the film composition follows the change of the feed ratio closely. Second, it appears that none of the plasma copolymer films has a long-chain linear $(CF_2)_n$ structure like that of conventional PTFE. In the structure of the plasma copolymer films, there are various proportions of CF_n structural units, and many other non-fluorine carbon components, such as aliphatic moieties, modified benzene rings, and even graphitic carbons, depending on processing conditions. The plasma copolymerization with OFCB and benzene involves polymerization, cross-linking, rearrangement, fragmentation, elimination, and ablation. There is strong competition among these reactions so that the resultant films are a complicated mixture of oligomers and polymer fragments, with a highly branched and cross-linked structure due to the complexity of the plasma polymerization. The detailed chemistry of these plasma homo-/copolymerizations will be discussed in a future publication.

Ellipsometry was used to characterize the optical properties of all homo- and copolymerized films. The nonlinear relationship between the feed ratio and the atomic composition ratio F/C in the plasma polymerized films is shown in Figure 3(a), and the linear dependence of the refractive index on the F/C ratio of each film is shown in Figure 3(b). All the experiments have good reproducibility, and sample-to-sample variation in the refractive index for a given composition was less than 3%. Figure 3 indicates that the copolymerization process results in films with a continuously varying refractive index. The measured RI values follow a linear relationship with F/C ratio for the homopolymerized and copolymerized films, as seen in Figure 3b. With increasing fluorine content in the plasma copolymerized films, the RI gradually decreases from 1.623 for the PP-benzene film to 1.368 for the PP-OFCB film. A small but finite absorption coefficient (not shown) over the same spectral range was measured and increased as the fluorine content increased. Therefore, the relationship between feed ratio and refractive index allows films with predictable refractive index profiles to be deposited.

To demonstrate the efficacy of this PECVD polymerization in the fabrication of highly constrained optical designs, AR coatings for common glass substrates {BK7 (n = 1.515) and F2 (Esco Products, n = 1.614)} of differing refractive index were fabricated. Single-layer AR coatings of MgF_2 (n = 1.38) are typically used for

(31) Limb, S. J.; Lau, K. K. S.; Edell, D. J.; Gleason, E. F.; Gleason, K. K. *Plasmas Polym.* **1999**, *4*, 21.
(32) Tibbitt, J. M.; Shen, M.; Bell, A. T. *J. Macromol. Sci., Chem.* **1976**, *A10*, 1623.
(33) Tanaka, K.; Yamabe, T.; Takeuchi, T.; Yoshizawa, K.; Nishio, S. *J. Appl. Phys.* **1991**, *70*, 5653.
(34) Durrant, S. F.; Mota, R. P.; de Moraes, M. A. B. *Thin Solid Films* **1992**, *220*, 295.
(35) Silverstein, R. M.; Webster, F. X. *Spectrometric Identification of Organic Compounds*; John Wiley and Sons: New York, 1998.

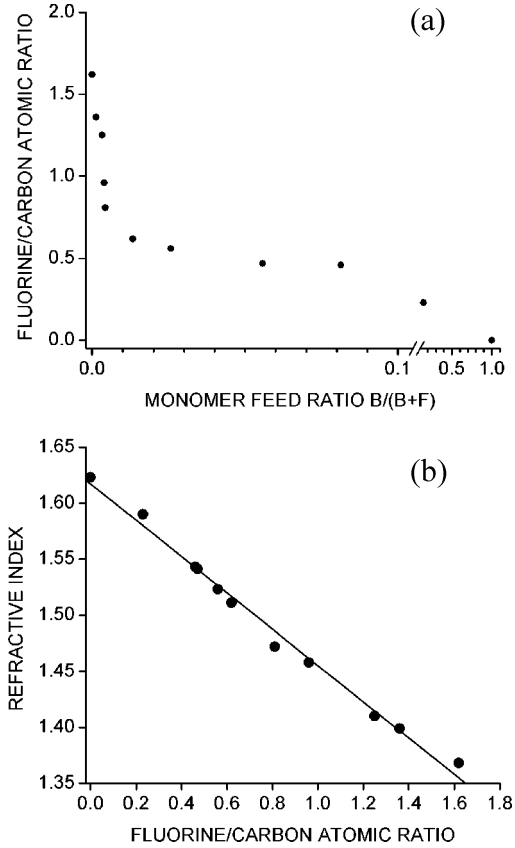

Figure 3. (a) Nonlinear relationship between the feed ratio and the fluorine/carbon atomic ratio in the plasma polymerized films, and (b) linear dependence of the refractive index (at 632.8 nm) on the composition ratio of each film. The F/C atomic ratio in the resultant films was determined by XPS.

Table 2. Design Specifications for 6-Layer AR Coatings for Two Different Substrates (the First Layer Contacts the Glass Wafer, and the Sixth Layer Contacts Air)

layer	BK7 glass RI	BK7 glass design thickness (nm)	F2 glass RI	F2 glass design thickness (nm)
first layer	1.515	22.9	1.614	51.6
second layer	1.492	23.3	1.569	34.3
third layer	1.453	24.6	1.495	34.4
fourth layer	1.411	24.6	1.421	34.4
fifth layer	1.379	25.2	1.376	34.4
sixth layer	1.367	25.4	1.367	17.1

visible light applications because the refractive index best approximates the ideal single-layer AR coating RI of $n = 1.22$ between air ($n = 1$) and a glass substrate ($n = 1.5$). These one-layer designs typically lack in capability across spectral regions. To obtain AR coatings with improved reflectance reduction and spectral performance (broader wavelength applicability), multilayer coatings are typically used where the individual layer thicknesses ($\ll$ optical wavelength) and refractive indices are systematically varied in a stepwise fashion from substrate to air. On the basis of the principles and model calculation described in the Experimental Section, an optimum six-layer AR coating, designed for BK7 ($n = 1.515$) and F2 (Esco Products, $n = 1.614$) utilizing subwavelength-thick plasma polymerized films of differing refractive indices, was chosen to demonstrate the capability to manipulate a GRIN profile and optical design flexibility. Table 2 lists the required thickness and

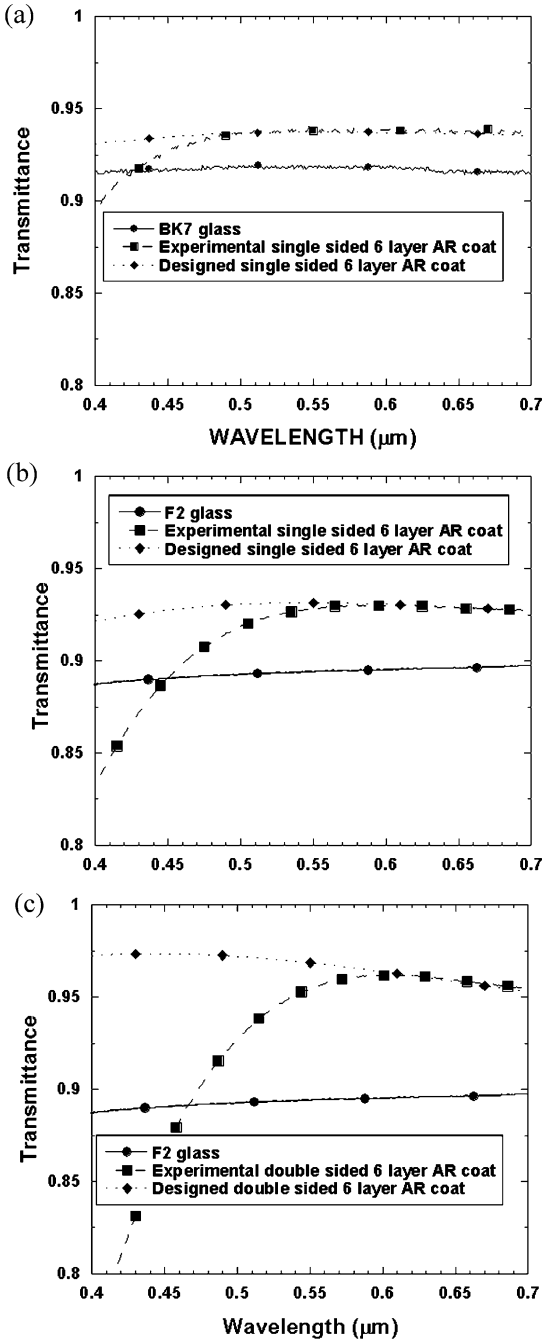

Figure 4. UV-Vis spectra data of a single-sided 6-layer antireflection film on (a) a BK7 substrate and (b) a F2 substrate, and (c) a double-sided 6-layer antireflection coating deposited on F2 glass. Please note the *y*-axis is highly expanded from 0.8 to 1.0 in transmittance.

refractive index of the six layers for each substrate. The AR coating on the BK7 glass substrate had steps of approximately equal physical thickness, as did the F2 glass substrate except for the first and last layer. For the F2 glass, the first layer was 1.5 times as thick as the second layer, and the last layer was half as thick as the fifth layer. In the designs, the refractive index of the first layer is the same as that of the glass substrates and the middle layers have gradually decreasing refractive indices. The outermost layer in each design was a PECVD OFCB homopolymer film with the lowest refractive index (1.368) in the series. Because the film thicknesses could not be measured in situ, respective film layers were grown to the appropriate thickness

using the previously determined individual growth rates (see Table 1). The following results demonstrate the success of this fabrication process.

Figure 4(a) and (b) show the transmission spectra of blank and one-side coated BK7 and F2 glasses, respectively. Fresnel reflections at both the top and bottom surfaces result in an overall transmission of approximately 91.8% for blank BK7 and 89.5% for blank F2. The F2 glass has a lower transmittance due to the higher reflection loss caused by its larger refractive index. Upon deposition of the six-layer AR coating shown in Table 2, part of the reflection loss across the visible area (400−700 nm) was minimized. Coating one side of the BK7 glass results in a transmission improvement to approximately 93.8%, and coating one-side of the F2 glass leads to a transmission increase to 93.0%. For both substrates, good agreement between the experimental transmission curves and the design models was observed. Below 450 nm, the difference between the experimental and the designed transmission is due to the small yet finite absorption coefficients of the films. To further improve the overall transmission, the same six-layer AR stack was applied to both sides of the F2 glass window; the design and experimental transmission results are shown in Figure 4(c). The design transmission of 96.4% at 600 nm was approached (96.2%) again demonstrating excellent accordance between the experimental test and theoretical prediction. These results demonstrate that PECVD is a simple, efficient, and environmentally friendly methodology to tailor polymer photonic elements with controllable optical properties. Plasma copolymerization of two or more monomers is capable of generating high-performance photon GRIN films on the nano-length scale with large refractive index variations ($\Delta n > 0.3$).

Acknowledgment. We acknowledge support from both the Air Force Research Laboratory and the Air Force Office of Scientific Research/NL.

CM035226Q